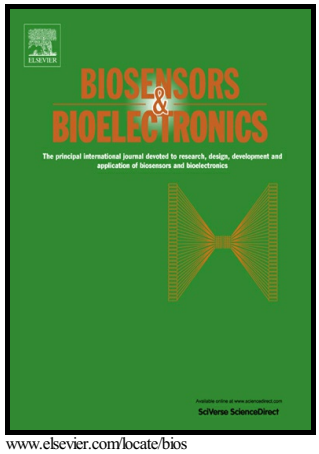

www.elsevier.com/locate/bios

BIOSENSING BREAST CANCER CELLS BASED ON A THREE-DIMENSIONAL TIO_2 NANOMEMBRANE TRANSDUCER

Fernando Zanghelini, Isaac A.M. Frías, Moacyr J.B.M. Rêgo, Maira G.R. Pitta, Marco Sacilloti, Maria D.L. Oliveira, Cesar A.S. Andrade

PII: S0956-5663(16)31148-4
DOI: http://dx.doi.org/10.1016/j.bios.2016.11.006
Reference: BIOS9325

To appear in: *Biosensors and Bioelectronic*

Received date: 25 August 2016
Revised date: 2 November 2016
Accepted date: 3 November 2016

Cite this article as: Fernando Zanghelini, Isaac A.M. Frías, Moacyr J.B.M. Rêgo Maira G.R. Pitta, Marco Sacilloti, Maria D.L. Oliveira and Cesar A.S. Andrade BIOSENSING BREAST CANCER CELLS BASED ON A THREE-DIMENSIONAL TIO_2 NANOMEMBRANE TRANSDUCER, *Biosensors an Bioelectronic,* http://dx.doi.org/10.1016/j.bios.2016.11.006

BIOSENSING BREAST CANCER CELLS BASED ON A THREE-DIMENSIONAL TIO_2 NANOMEMBRANE TRANSDUCER

Fernando Zanghelini[1], Isaac A. M. Frías[1], Moacyr J.B.M. Rêgo[1], Maira G.R. Pitta[1], Marco Sacilloti[2], Maria D.L. Oliveira[3], Cesar A.S. Andrade[1,3*]

[1]Programa de Pós-Graduação em Inovação Terapêutica, Universidade Federal de Pernambuco, 50670-901 Recife, PE, Brasil

[2]Departamento de Física, Universidade Federal de Pernambuco, 50670-901 Recife, PE, Brasil

[3]Departamento de Bioquímica, Universidade Federal de Pernambuco, 50670-901 Recife, PE, Brasil

[*]Corresponding author: Departamento de Bioquímica, Universidade Federal de Pernambuco, 50670-901 Recife, PE, Brasil. Tel.: +55 81 2126.8450; fax: +55 81 2126.8576. csrandrade@gmail.com

Abstract

The early diagnosis of breast cancer is crucial for the successful treatment and recovery phases of the patients suffering from the disease. Although mammography is considered the gold standard for diagnosis, it fails to detect some cancers in high-density breasts. In this work, we propose for the first time a tridimensional biosensor platform, to be used on an electrochemical point-of-care device. The bioconjugated platform is constructed on a series of covalent linkages between lectin molecules and a cysteine layer immobilized over gold-coated TiO_2 butterfly-like tridimensional nanomembranes. Through the use of vegetal lectins, we managed to take advantage of the markedly atypical glycomic profile of the cancerous mammalian cell membrane and successfully made a distinction between highly invasive (T47D) and less invasive (MCF7) cancer

cell lines. The selectivity of the biosensor was tested by using normal human skin-fibroblast. The proposed cytosensor demonstrated limits of detection as low as 10 cells mL^{-1} for every cell line and a linear range from 10 to 1.0×10^6 cells mL^{-1}. Considering that electrochemical impedance values can be correlated with the number of breast cancer cells present in the sample, we suggest that the proposed platform could be useful in facilitating the diagnosis of cancer.

Keywords: cancer cells; biosensor; lectins; impedance spectroscopy.

1. Introduction

Unlike triple-negative breast cancer, which is known to lack the expression of estrogen and progesterone receptors (Petrelli et al. 2014), the diagnosis of other primary breast cancers is quite difficult. Because breast cancer is the primary cause of death among women worldwide (Diaby et al. 2015), it is important to develop alternatives to help diagnose breast cancer subgroups. Fortunately, today well-known and characterized tumor-derived mammary epithelial cell lines are available that can serve as models in evaluating the efficiency and specificity of innovative diagnostic platforms. Based on distinct attributes such as their gene expression levels, *in vitro* growth and their *in vivo* tumorigenic and metastatic capabilities (Zajchowski et al. 2001), cell lines such as MDA231, MDA435 and T47D have been classified as highly invasive, while other breast cancer cell lines such as MCF7, MDA453 and SKBR3 are recognized as weakly invasive. T47D and MCF7 are two cancer cell lines that simultaneously express estrogen receptor (ER) and progesterone receptor (PgR) (Holliday and Speirs 2011; Pellegrini et al. 1995). The abnormal expression rate of these receptors on each cell line represents a unique fingerprint constituted by different

extracellular and intracellular molecules such as glycoproteins, proteins and nucleic acid aptamers, peptides and glycans.

In the last five years, it has been demonstrated that the differentiation of diverse cancer cell lines can be achieved by constructing a glycomic profile based on the markedly atypical glycosylation of the cancerous mammalian cell membrane (Drake et al. 2010; Hua et al. 2014). Hence, employing the extracellular glycan fingerprint, a kind of glycoprotein, to differentiate breast cancer subtypes is a convenient alternative that obviates the use of animals for the production of antibodies. Additionally, high-throughput techniques sometimes require labeling antibodies with large signaling molecules that decrease their immune recognition activity (Yang et al. 2015).

Lectins are another group of ubiquitous proteins or glycoproteins extracted from plants or animals. They bind strongly to specific glycan moieties found on the surface of the cell membrane (Bertrand et al. 2014). Because of their stability and ease of extraction, lectins have been used in many of the early clinical cancer biomarker tests to detect the carcinoembryonic antigen, colorectal cancer and the prostate specific antigen (Hammarström 1999; Meany et al. 2009; van Gisbergen et al. 2005). Currently, there are several protocols that employ single or multiple lectins, such as Concanavalin A (ConA), Wheat germ agglutinin (WGA), *Aleuria aurantia* lectin, *Lens culinaris* agglutinin, *Lycopersicon esculentum* lectin among others, to capture specific glycoproteins and glycopeptides (Drake et al. 2010).

In general, after traditional biopsy, the challenge to classify the invasiveness of breast cancer is an traumatic experience not only for the health services, but also for the patient. The collected sample is usually tested by clinical immunoassays such as immunohistochemistry or fluorescent *in situ* hybridization and chromogenic *in situ* hybridization; however an inconclusive result is by no means uncommon (Hua et al.

2014). The accumulation of knowledge on the behavior of different breast cancer subgroups has encouraged efforts to develop faster, easier and cheaper differentiation platforms in the form of biosensors (Arif et al. 2015; Benvidi et al. 2015; Thiagarajan et al. 2016). Over the last ten years, optical, piezoelectric and electroanalytical transducers have been preferred for fabricating breast cancer immunological biosensors (Arkan et al. 2015; Kosa et al. 2013; Liu et al. 2014; Lucarelli et al. 2008). Nanoscale materials and structures based on conducting polymers and semiconductors (Ali et al. 2015; Arkan et al. 2015; Liu et al. 2014) are used on the recognition ligand or as labels but, their working principle still based on ELISA methodology (Huber et al. 2015). Among the most reported analytical techniques, electrochemical impedance spectroscopy (EIS) is recognized for being a sensitive label-free methodology.

Biosensors developed for the selective detection of cells using electrochemical techniques are known as electrochemical cytosensors. For the most part, they are designed to identify cancer cells and are considered practical and robust. Several electrochemical cytosensors have been appropriately modified to be selective towards cervical cancer (HeLa) and leukemia (Tepeli et al. 2016; Tepeli et al. 2015). Zhu et al. detailed an electrochemical cytosensor based on human epidermal growth factor receptor 2, which is overexpressed in some breast cancer cells. They obtained a limit of detection (LOD) of 26 cells mL^{-1}. LOD was determined based on the standard deviation (S.D.) of response and calculated slope LOD = $3.3\sigma/s$ (s is the slope of the calibration curve and σ is the S.D. of response). In this work, we developed a lectin-based biological sensor that allows us to differentiate between a normal human skin-fibroblast (NHSF) cell line and a less invasive MCF-7 and more invasive T47D cancer cell lines by means of their outer-membrane carbohydrate profile. With this cytosensor, we obtained a LOD of 10 cells mL^{-1} and a linear range from 10 to 1.0×10^6 cells mL^{-1}.

TiO_2 butterfly-like membrane nanostructures (TiO_2-MN) were grown by means of the metal-organic chemical vapor phase deposition (MOCVD) method (Lazar et al. 2008) and used as the electrochemical platform. Since this nanomaterial is known for its non-linear optical properties (Dominguez et al. 2012), we recognize that our methodology has the potential to be simultaneously verified as an optical transducer. Even though other metal oxides such as ZnO exhibit a higher electron mobility and diffusion coefficient (Ali et al. 2015), TiO_2 is known for its minimal protein denaturation activity, excellent biocompatibility and chemical and photochemical stability (Derkus et al. 2014).

The exceptional electrochemical and catalytic properties of metal nanoparticles dispersed over a metal oxide substrate are well documented (Li and Tang 2014). Furthermore, the prospective use of intradermal biosensors highlights the need for biocompatible and chemically stable materials. TiO_2 is a distinctive material that not only gathers these requirements but also allows the manipulation of its shape at the nanoscale. The use of nanostructures as electrochemical platforms has demonstrated their ability to lower the detection limits below those of conventional non-modified gold-disc electrodes (Sage et al. 2014). By means of nanotechnologies, such as MOCVD, we succeeded in shaping butterfly-like micrometrical TiO_2 structures whose wings are detailed on the nanometer scale. The peculiar shape of these structures enables the enhancement of an important deriving lattice effect that allows us to construct a robust electrochemical platform. According to computational calculations and experimental results (Tong et al. 2010; Wang et al. 2013), freshly synthesized TiO_2 contains oxygen atoms located at different border positions, namely bridged oxygen atoms, in-plane oxygen atoms and oxygen vacancies resulting from the 5-fold and 6-fold coordinated Ti atoms. Oxygen vacancies are most likely to occur on TiO_2 lattice

defects, which are found in abundance on our TiO_2-NM structures. The prompt subsequent vaporization of gold provides the rapid sintering of Au^+ atoms onto oxygen vacancies. As a result, the deposited gold film remains strongly bound to the O^- defects at the interface through apical Au atoms. The robust attachment of the gold film to the TiO_2-NM structures provides an excellent platform for the subsequent cystein-lectin modification.

We emphasize that the efforts of our group are intended to explore an environmentally friendly functionalization of the TiO_2-NM transducer while maintaining its biocompatibility and simultaneously, enhancing its sensitivity. In this sense, despite the fact that 3D-patterned electrode intrinsically improves the electrochemical response of the cytosensor, the gold-coated surface provides additional benefits. For instance, the adoption of the gold film covering the three dimensional transducer allows the subsequent tethering of multiple ligands, cysteine and lectins. In this manner, multivalency governs the binding affinities of the tethered ligands, enhancing analyte capturing by orders of magnitude (Fukui et al. 2002; Mulder et al. 2004). Furthermore, the incorporation of gold clusters and films creates synergistic functional devices combining molecular functionality with redox and electronic activity (Chandrasekharan and Kamat 2000; Drechsler et al. 2004; Subramanian et al. 2004). Hence, the redox response of our TiO_2-NM biosensor becomes largely discernable. Shi et al. found a similar effect after gold nanoparticles were assembled on a nanostructured TiO_2 film, resulting in a better conductivity than that of the nano-TiO_2 film alone (Shi et al. 2007). In addition, in our experience (Luna et al. 2015; Oliveira et al. 2011; Simão et al. 2016), the use of cysteine serves as an efficient spacer for the motility of the redox probe and as a stable linker towards lectins, antibodies and aptamers. We compared the electrochemical response of TiO_2-MN conjugated with that of ConA, which has a broad

reactivity towards the mannose moieties found on N-linked glycans, to that of TiO_2-MN conjugated with wheat germ agglutinin (WGA), which presents affinity towards cells via the specific binding capacity to the N-acetylglucosamin (GlcNAc) found on N-glycans of the cell surface.

2. Materials and Methods

2.1. Materials

Bovine serum albumin (BSA), RPMI 1640 medium, phosphate buffered saline (PBS), ConA, WGA, cysteine (Cys), 1-ethyl-3-(3-dimethylaminopropyl) carbodiimide (EDC) and N-hydroxysuccinimide (NHS), Titanium (IV) isopropoxide $Ti(OC_3H_7)_4$ (99.999%) and Ferrocene $Fe(C_5H_5)_2$ (98%) were obtained from Sigma Chemical Co. (St Louis, USA) and used as received. Potassium ferri- and ferrocyanide were obtained from VETEC (Brazil). All chemicals and solvents were of analytical grade and used as received, without further purification. All water used in the experiments was obtained from a Milli-Q plus (Billerica, USA) purification system.

The NHSF from the CCDSK cell line and breast-cancer cell lines (MCF-7 and T47D) were obtained from Rio de Janeiro Cell bank (BCRJ, Federal University of Rio de Janeiro, Brazil). The cells were cultured in RPMI 1640 supplemented with 10% fetal bovine serum, 2 mM glutamine, 100 mg mL^{-1} streptomycin, and 100 U mL^{-1} penicillin at 37 °C with 5 % CO_2 (Samoszuk et al. 2005). In this study, cells with a passage number lower than 30 were employed for all *in vitro* experiments. Trypsinization of cell cultures was carried out with 1.0% trypsin to dissociate the adhered cells, which were counted and adjusted to a known number of cells. For the biosensing investigation, the cell suspensions were centrifuged at 3000 rpm for 5 min and then washed twice with

PBS, following which the TiO_2-MN-lectin electrode was immersed in the cell suspensions for 30 min.

2.2. Instruments

A quick coater-SC-701 (Sanyo Electronics, Tokyo, Japan) sputtering device was used to evaporate a thin layer of gold over the nanostructured surface to allow lectin immobilization and also to prepare microscopy samples. Morphological characterization of the nanostructured substrate was performed using a scanning electron microscope (SEM) JSM 5900 electron microscope (JEOL Instruments, Japan). The scan length, working distance and magnification were adjusted to obtain adequate resolution.

The electrochemical experiments were performed on a three-electrode cell using a PGSTAT 128N potentiostat/galvanostat (Autolab, Eco Chemie, The Netherlands). TiO_2-MN nanostructured surface was used as the working electrode while platinum wire and Ag/AgCl saturated with KCl were used, respectively, as counter and reference electrodes. Current vs. voltage measurements were carried out at a 50 mVs^{-1} scan rate and a potential ranging from - 0.2 to + 0.7 V was used. Impedance measurements were recorded between 100 mHz to 100 kHz frequency range. The amplitude of the applied sine wave potential was 10 mV. The electrochemical measurements were carried out at different stages during the preparation of the nanostructured substrate and performed when immersed in a 10 mM $K_4[Fe(CN)_6]^{4-}/K_3[Fe(CN)_6]^{3-}$ (1:1, v/v) redox probe solution buffered in PBS at pH 7.4. All electrochemical measurements were repeated in triplicate and carried out at room temperature inside a Faraday cage.

2.3. Sensor Fabrication

2.3.1. Growth of three-dimensional TiO_2 nanostructures

The TiO_2-MN were prepared according to a previously reported method (Fabreguette et al. 2001; Lazar et al. 2011; Lazar et al. 2008), with a slight modification of the substrate thickness and TiO_2-MN growth temperature. Briefly, a 5-nm thick cobalt film was obtained using the electron beam physical vapor deposition method on soda lime glass substrate. The film was then annealed at 500 ºC for 1 hour under atmospheric air conditions. The TiO_2 structures were grown in a horizontal geometry home-made MOCVD reactor operating under 76 torr with a growth temperature of 550 ºC, using N_2 as carrier gas (0.6 slm-standard litres per minute), $Ti(OC_3H_7)_4$ as the source for both Ti and O, and $Fe(C_5H_5)_2$ as the catalyst. These were the only fixed conditions set for growth pressure and carrier gas flow.

2.3.2. Modification of the TiO_2-MN nanostructured surface

In order to achieve strong bonding between lectins and TiO_2-MN, a 10 nm gold layer was evaporated on top of TiO_2-MN, to which 5 µL of Cys solution (30 mM) was subsequently added. Cys amino acid anchors through gold-thiolate bonding to the nanostructured surface and, simultaneously, will serve as the immobilizer for lectins. After a waiting time of 15 min, we rinsed the surface with generous amounts of PBS buffer solution to remove any non-linked molecules. Thereafter, the Cys-modified TiO_2-MN electrode surface was treated with a 0.4 M EDC and 0.1 M NHS (1:1, v/v) solution for 10 min to activate the terminal carboxylic group of Cys (Andrade et al.). After this period, the surface was treated for 10 min with 5 µL of lectin solution to establish terminal covalent linkages. Finally, bovine serum albumin was used to block the remaining active sites. The procedure described provides the transducer with a strong immobilization of the bio recognition layer as a result of the subsequent covalent

anchoring of the lectins. The sensing ability of the platform towards cancerous cells was assessed by testing solutions at different cell concentrations, between 10 and 10^6 cells. NHSF cell line solution was employed as a negative sample.

3. Results and discussion

3.1 Morphological studies

The proposed strategy to differentiate breast cancer cells according to their outer-membrane glycomic profile is illustrated in Fig. S1. The process to fabricate the biosensor was monitored by scanning electron microscopy. Fig. 1a shows a SEM micrograph of the pristine substrate after TiO_2-MN growth. We note a growth tight and homogeneous arrangement of the nanostructures over the glass. In Fig. 1b, we present a single membrane-like structure of TiO_2-MN after immobilizing the Cys layer on its surface. The wing-like morphology is evident. Fig. 1c shows a micrograph of a single membrane nanostructure after its modification with WGA. In this step, a large amount of aggregates is clearly visualized, a result that suggests the successful immobilization of lectins. We attribute the presence of these lectin-agglomerates to the impedance increment found in our results obtained by EIS measurements.

In order to facilitate the understanding of the biorecognition event, we performed SEM microscopy of the electrodes before the electrochemical measurements (Fig. 2). In these samples, 10^6 cell solutions were employed. The electrodes were exposed to the cell solution for 30 min. After rinsing out the unbounded cells, the electrodes were treated with a 2.5% glutaraldehyde solution for 1 h at 4 °C to fix the cells and make them resistant to metallization and SEM microscopy (Chen et al. 2016). In Fig 2a we observe a greater amount of MCF7 cells adhered to the electrode. This

amazing behavior is the result of ConA modification of TiO_2-NM structures. The greatest responses were observed for ConA recognizing MCF7 and T47D (Figs. 2a and 2c). On the other hand, we noticed a lower amount of MCF7 and T47D cells adhered to the WGA-modified electrodes (Figs. 2b and 2d). When NHF were tested, we noticed that a small amount of cells were adhered to them. However, they are bigger than breast cancer cell lines, which accounts for their electrochemical response. These results are in accordance with our electrochemical measurements.

3.2 Electrochemical Impedance Spectroscopy

EIS was conducted to study the behavior of the platform before and after each modification step of the electrode surface and to quantify the affinity of each cell line towards a specific lectin. The methodology employed can be found in section *2.2*. The TiO_2-MN-modified electrode surface (Fig. 3a) showed a process limited by diffusion that reveals its conductive nature, which improves sensor sensitivity. A better conductivity was observed for nano-TiO_2 after the evaporation of a thin gold film on its surface improved the detection limit of the biosensor (Fig. 3a). Similar results have been obtained by other authors (Shi et al. 2007). A modified Randles equivalent circuit was adopted to analyse TiO_2-MN behavior and sensor performance. The Randles circuit includes the ohmic resistance of the electrolyte solution (R_Ω), Warburg impedance (W) resulting from ion diffusion from the bulk electrolyte to the electrode interface, phase constant element (Q), and the charge-transfer resistance (R_{CT}) recognized when the electrolyte solution contains a redox probe. The diameter of a Nyquist semicircle is related to R_{CT}.

Table S1 shows the electrical parameters calculated from the mathematical fitting of EIS responses. The TiO_2-MN-lectin mounting procedure and interactions between WGA or ConA with the glycomic profile of the chosen cell lines are presented.

Fig. 4 shows the stepwise nature of the TiO_2-MN-lectin electrode modification and ConA/WGA interaction with different cancer cell lines (MCF7, T47D and NHSF). An increase can be observed in the R_{CT} values after immobilization of ConA (0.80×10^6 Ω) and WGA (2.56×10^3 Ω) at the TiO_2-MN modified electrode. The impedimetric response to WGA was lower than ConA, owing to the molecular weight and tridimensional structure of these lectins. ConA presents a tetramer conformational distribution that influences the adsorption process at the electrode surface and the end of the electrochemical responses (Oliveira et al. 2008). Bovine serum albumin was used to block the remaining actives sites at the electrode surface and, as expected, promotes an increase in the R_{CT} after adsorption.

In addition, TiO_2-MN-ConA and TiO_2-MN-WGA revealed a good interaction with tested cancer cell lines. As expected, cancer cell systems in a malignant phenotype are associated with a variety of altered cell glycosylation patterns. These carbohydrate patterns are observed in glycolipids, glycosphingolipids and glycoproteins (Goetz et al. 2009). In addition, structural information indicates that the carbohydrate-binding activity of most lectins was generated by limited amino acid residues designated as the carbohydrate recognition domain (CRD). In fact, CRD typically recognizes the terminal non reducing carbohydrate residues of cell membrane glycoproteins and glycolipids (Mody et al. 1995). The TiO_2-MN-WGA system demonstrated the best response to T47D line ($R_{CT} = 15.0 \times 10^3$ Ω) when compared to the MCF7 line ($R_{CT} = 4.5 \times 10^3$ Ω).

It is note that T47D is composed of a simple glycosylation pattern, with NeuAcα2–3Galβ1-3GalNAc-ol, Galβ1-3GalNAc-ol, and GalNAc-ol predominating

(Lloyd et al. 1996). These characteristics are an important key factor involved in the WGA response against the T47D line. In addition, WGA binds with high affinity to internal GlcNAc residues in large oligosaccharides containing repeat sequences of Gal β(1-4)GlcNAc β(1-3) that reinforce the R_{CT} response obtained in the impedimetric analysis (Gallagher et al. 1985).

MCF7 cells are hypoglycosylated tumors that resulting directly in a lower impedimetric response (Engelmann et al. 2008). In addition, a previous study revealed that MCF7 have high-mannose structures with dominant high-mannose glycans (Man5-9GlcNAc2) accompanied by less abundant fucosylated tri- and tetrantennary higher sialylated glycans that promote ConA carbohydrate recognition (Lattová et al. 2011; Lattova et al. 2010). ConA is a Gly/Man specific lectin, and is a tetramer at physiological pH, with each monomer possessing one saccharide site as well as a metal ion site (Bhattacharyya et al. 1991). The TiO_2-MN-ConA system (Fig. 4d) revealed an important impedimetric response for the MCF7 line. This behavior is associated with ConA sugar recognition and previous studies have shown biological activities to interact with different glycoproteins present in human plasma (Lima et al. 1997), and a selective response to normal and transformed human mammary cells (Beltrao et al. 1998).

Results for the interaction between the NHSF cell line and lectins (WGA or ConA) showed lower R_{CT} and n values, which corresponds to a smaller blocking effect of the biosensor surface associated with a smaller capacitive dispersion. Q and n are constant phase element parameters, and these elements are associated with the reactance and dispersion of the constant phase element, respectively. Our results provided information on the variation of n. This parameter is close to 1 in most experiments, and close to 0.5 only for the TiO_2-MN-lectin-modified electrode recognizing NHSF cells.

This is an indication of a number of diffusional aspects of the charge transfer process in the interface. These results indicate diffusional limitations present in the material immobilized on the electrode surface. In addition, some authors have highlighted that roughness (de Levie 1965), fractal geometry of surface (Nyikos and Pajkossy 1985), adsorption (Pajkossy 1997), 2D and 3D geometric distributions (Jorcin et al. 2006) and heterogeneities in the atomic scale (Bouckaert et al. 2000) can influence n values.

Among other impedance components, the changes in R_{CT} were the most significant. Electrode surface modifications affect the Rct element due to a blockage in the electron transfer resulting in a decrease in the permeability decrease of the redox probe system at the interface. It can be seen that, in general, the charge transfer resistances for systems with ConA are larger than those with WGA. The sequence of TiO_2-MN, TiO_2-MN-lectin, and TiO_2-MN-lectin-cells-modified electrode measurements, approximately shows the additive blockage of the interface, confirming that the amount of material immobilized and/or adsorbed on the electrode surface directly correlates with the impedance (diameter of semicircle). Our results demonstrate that these lectins retain their capability for recognition after exposition on the electrode surface. The differences in the dielectric responses are due to the monosaccharide-binding site of the ConA and WGA lectins.

A nonsignificant bioaggregation between lectin and NHSF cells, due to the saccharide profile on the surface of the latter is also of note. A lower response is observed because all mammal cells express sialic acids and other glycan chains on the surface of their outer membrane. In fact, a normal human cell membrane such as NHSF has more than 10 million glycan molecules on its outer cell membrane (Varki and Schauer 2009). It is worthy of note that NHSF cells are composed mainly of galactose and sialic acid (Tsay et al. 1975).

In addition, the response obtained for the WGA-modified electrode is higher when it is exposed to the T47D (more invasive) as compared to the MCF7 (less invasive) cell line. Specific changes occur during the tumorigenic process in addition to the accumulation of N-acetyl glucosamine, particularly, switches and changes in glycan linkages (Varki and Schauer 2009). These modifications are related to the more invasive characteristic present on the T47D cell line. On the other hand, we found an even greater response for the ConA sensor against the cancer cell line, since its lectin binds directly to the mannose moieties present in all types of N-linked glycans.

The results presented in Figure 4 clearly show that both lectins were able to recognize altered carbohydrates present at cancer cell lines, as can be seen by the increase in the R_{CT}. Since this resistive component controls the charge transfer kinetics of the redox probe at the electrode interface, its value will vary according to the amount of cells adsorbed on the electrode surface. For this reason, we used $\Delta R_{CT}\%$ to evaluate the sensitivity of our biosensor through the linearity of the collected responses at each cancer cell concentration, as follows $\Delta R_{CT}\% = \left(\frac{R_{CT}^{Lectin} - R_{CT}^{Cell\ line}}{R_{CT}^{Lectin}}\right) \times 100$. R_{CT}(Lectin) is the value of the charge-transfer resistance of the TiO_2-MN-lectin-modified electrode and R_{CT}(Cell line) is the value of the charge-transfer resistance of the TiO_2-MN-lectin platform after exposure to a solution containing different concentrations of MCF-7, T47D or NHSF cells.

As can been seen, a study was carried out for different cell concentrations. A more detailed analysis that summarizes the interaction between the glycomic profile of the cells and the selected lectins is shown in Figure 5. ΔR_{CT} clearly increases with cell concentration. The ΔR_{CT} response indicated that the interactions between lectins and cancer cells can be sensed by the modified electrode. The increase in the ΔR_{CT} is different for both lectins; however, for higher cell concentrations, ConA and WGA

showed a higher ΔR_{CT} (Fig. 5). We observed that lower changes in electron-transfer resistance were detected with experiments using NHSF cells. The fact that both lectins are known to have different interactions with carbohydrates in normal and cancer cells, indicates that the changes in electron-transfer resistance observed with cancer cell sugar were due to a specific lectin-sugar interaction.

The biorecognition capacity of lectins was evaluated based on inhibition of the binding sites.Specific sugars such as glucose and N-acetylglucosamine were then used to inhibit ConA- and WGA-specific sites, respectively (Liu et al. 2016; Sadik and Yan 2007). As can be seen in supplementary material (Fig. S2), following contact of the biosensor with carbohydrates, an increase in the R_{CT} was observed due to the biointeraction process. Subsequently, these modified systems were exposed to MCF-7 and T47D cell lines. As expected, no significant responses were observed during the impedimetric response.

Table S2 shows the results for the quantitative assay of cell lines associated with the biointeraction occurring between the ConA and WGA lectins and the MCF-7, T47D and NHSF cell lines. Based on cell-based biosensors reported in the literature (Table 1), we confirmed that the proposed biosensor performed well for the detection of breast cancer cells with wide linear ranges and low detection limits. These interesting results suggest that the biorecognition ability of the lectin was preserved after the immobilization. Furthermore, the proposed sensing platform used in conjunction with EIS showed a high sensitivity and specificity. Our biosensors were able to discriminate and quantify cancerous cells from real breast tissue samples, suggesting a potential application in cancer diagnosis.

Conclusions

This work presented the construction of a tridimensional bio-recognition layer achieved through covalent linkages between gold-cysteine and the further covalent attachment of lectins. ConA has a broad reactivity for the mannose moieties found on N-linked glycans and WGA has specific affinity for N-acetylglucosamine (GlcNAc) of N-glycans occurring on the cell surface. The different specificities of each lectin allowed the recognition and differentiation of highly invasive cancer cell lines from weakly invasive cell lines and normal tissue cells. Our results demonstrated that the use of the TiO_2-MN-ConA-modified electrode provides excellent reproducibility and selectivity towards T47D cell line. The proposed approach demonstrated detection limits as low as 10 cells mL^{-1} and a linear range from 10 to 1.0×10^6 cells mL^{-1}. Because the constructed platform successfully quantified cancer cells, it could be employed to facilitate the diagnosis in the early stages of cancer. Furthermore, because untypical glycomic profiles are also associated with degenerative diseases and neurological disorders, these kinds of lectin-based biosensors may serve to explore the nature of the alkynyl sugars overlying the membrane of the affected cells.

Acknowledgments

The authors are grateful for support from the Rede de Nanobiotecnologia/CAPES, INCT_IF (Instituto Nacional de Ciência e Tecnologia para Inovação Farmacêutica), CNPq (grant 302885/2015-3 and 302930/2015-9) and FACEPE. Zanghelini and Frias would like to thank CAPES for a PhD and postdoctoral scholarships, respectively. Sacilotti would like to thank MCT-Cetene for grants related to scholarships.

Figure 1. SEM micrographs of TiO_2-MN (a), TiO_2-MN modified with cystein (b) and TiO_2-MN modified with WGA(c).

Figure 2. SEM micrographs of TiO_2-MN-ConA exposed to T47D (a), TiO_2-MN-WGA exposed to MCF7 (b), TiO_2-MN-ConA exposed to MCF7 (c), TiO_2-MN-WGA exposed to T47D (d), TiO_2-MN-ConA exposed to NHSF (e) and TiO_2-MN-WGA exposed to NHSF (f).

Figure 3. Electrochemical response of the TiO_2 butterfly-like tridimensional nanomembranes (a) and Randles equivalent circuit (b).

Figure 4. Electrochemical responses after testing different cell concentrations from 10 cells mL^{-1} to 1×10^6 cells mL^{-1}. (a) TiO_2-MN-WGA exposed to MCF-7, (b) TiO_2-MN-WGA exposed to T47D, (c) TiO_2-MN-ConA exposed to MCF-7, (d) TiO_2-MN-ConA exposed to T47D, (e) TiO_2-MN-WGA exposed to NHSF, and (f) TiO_2-MN-ConA exposed to NHSF.

Figure 5. ΔR_{CT}% for the TiO_2-MN-lectin modified electrodes after exposure to different cell concentrations of MCDF-7, T47D and NHFS.

Table 1. Comparison with other published cancer cell sensors.

Technique	Transducer	Cell lineage	Linear range (cells mL^{-1})	Limit of detection (cells mL^{-1})	Reference
CV,EIS	Thiolated sgc8c-DNA aptamer onto gold disc.	CCRF-CEM	1.0×10^4 to 1.0×10^7	6.0×10^3	(Pan et al. 2009)
CV	Glass carbon-MWNT-Au-ConA	A549	3.0×10^4 to 3.0×10^7	7.0×10^3	(Zhang et al. 2010)
		H1299	3.0×10^5 to 3.0×10^8	8.0×10^4	
		95-D	2.5×10^5 to 2.5×10^8	7.0×10^4	

		QGY-7701	3.6×10^5 to 3.6×10^8	1.1×10^5	
		QGY-7703	10 to 1.0×10^6	5.0	
		LNCaP	2.0×10^5 to 5.0×10^8	5.0×10^4	
EIS	TiO_2 MN-Gold Cys-ConA	T47D	10 to 1.0×10^6	10.0	This Work
		MCF7	10 to 1.0×10^6	10.0	
		NHSF	10 to 1.0×10^6	10.0	
	TiO_2 MN-Gold Cys-WGA	T47D	10 to 1.0×10^6	10.0	
		MCF7	10 to 1.0×10^6	100.0	
		NHSF	10 to 1.0×10^6	10.0	

References

Ali, M.A., Mondal, K., Singh, C., Dhar Malhotra, B., Sharma, A., 2015. Nanoscale 7(16), 7234-7245.

Andrade, C.A.S., Nascimento, J.M., Oliveira, I.S., de Oliveira, C.V.J., de Melo, C.P., Franco, O.L., Oliveira, M.D.L., 2015. Coll. Surf. B: Biointerf. 135(1) 833–839.

Arif, S., Qudsia, S., Urooj, S., Chaudry, N., Arshad, A., Andleeb, S., 2015. Biosens. Bioelectron. 65, 62-70.

Arkan, E., Saber, R., Karimi, Z., Shamsipur, M., 2015. Anal. Chim. Acta 874, 66-74.

Beltrao, E.I., Correia, M.T., Figueredo-Silva, J., Coelho, L.C., 1998. Appl. Biochem. Biotechnol. 74(3), 125-134.

Benvidi, A., Dehghani Firouzabadi, A., Dehghan Tezerjani, M., Moshtaghiun, S.M., Mazloum-Ardakani, M., Ansarin, A., 2015. J. Electroanal. Chem. 750, 57-64.

Bertrand, N., Wu, J., Xu, X., Kamaly, N., Farokhzad, O.C., 2014. Adv. Drug Deliv. Rev. 66, 2-25.

Bhattacharyya, L., Koenig, S.H., Brown, R.D., 3rd, Brewer, C.F., 1991. J. Biol. Chem. 266(15), 9835-9840.

Bouckaert, J., Dewallef, Y., Poortmans, F., Wyns, L., Loris, R., 2000. J. Biol. Chem. 275, 19778.

Chandrasekharan, N., Kamat, P.V., 2000. J. Phys. Chem. B 104(46), 10851-10857.

Chen, S., Goode, A.E., Skepper, J.N., Thorley, A.J., Seiffert, J.M., Chung, K.F., Tetley, T.D., Shaffer, M.S.P., Ryan, M.P., Porter, A.E., 2016. J. Microsc. 261(2), 157-166.

de Levie, R., 1965. Electrochim. Acta 10, 113.

Derkus, B., Cebesoy Emregul, K., Mazi, H., Emregul, E., Yumak, T., Sinag, A., 2014. Bioproc. Biosyst. Eng. 37(5), 965-976.

Diaby, V., Tawk, R., Sanogo, V., Xiao, H., Montero, A., 2015. Breast Canc. Res. Treat. 151(1), 27-40.

Dominguez, C.T., Lacroute, Y., Chaumont, D., Sacilotti, M., de Araújo, C.B., Gomes, A.S.L., 2012. Optics Express 20(16), 17380-17385.

Drake, P.M., Cho, W., Li, B., Prakobphol, A., Johansen, E., Anderson, N.L., Regnier, F.E., Gibson, B.W., Fisher, S.J., 2010. Clin. Chem. 56(2), 223-236.

Engelmann, K., Shen, H., Finn, O.J., 2008. Cancer Res. 68(7), 2419-2426.

Fabreguette, F., Guillot, J., Cardoso, L.P., Marcon, R., Imhoff, L., Marco de Lucas, M.C., Sibillot, P., Bourgeois, S., Dufour, P., Sacilotti, M., 2001. Thin Sol. Films 400(1–2), 125-129.

Gallagher, J.T., Morris, A., Dexter, T.M., 1985. Biochem. J. 231(1), 115-122.

Goetz, J.A., Mechref, Y., Kang, P., Jeng, M.H., Novotny, M.V., 2009. Glycoconj. J. 26(2), 117-131.

Hammarström, S., 1999. Semin. Cancer Biol. 9(2), 67-81.

Holliday, D.L., Speirs, V., 2011. Breast Cancer Res.: BCR 13(4), 215-215.

Hua, S., Saunders, M., Dimapasoc, L.M., Jeong, S.H., Kim, B.J., Kim, S., So, M., Lee, K.-S., Kim, J.H., Lam, K.S., Lebrilla, C.B., An, H.J., 2014. J. Proteome Res. 13(2), 961-968.

Huber, F., Lang, H.P., Zhang, J., Rimoldi, D., Gerber, C., 2015. Wiss Med Wkly 145, w14092.

Jorcin, J.B., Orazem, M.E., Pébère, N., Tribollet, B., 2006. Electrochim. Acta 51, 1473.

Kosa, C., Kardos, L., Kovacs, J., Szollosi, Z., 2013. Pathol. Res. Pract. 209(3), 147-150.

Lattová, E., Bartusik, D., Spicer, V., Jellusova, J., Perreault, H., Tomanek, B., 2011. Mol. Cell Proteomics 10(9), M111.007765.

Lattova, E., Tomanek, B., Bartusik, D., Perreault, H., 2010. J. Proteome Res. 9(3), 1533-1540.

Lazar, M., Chaumont, D., Lacroute, Y., Chassagnon, R., Ciobanu, I., Sacilotti, M., 2011. Sci. Adv. Mater. 3(1), 102-106.

Lazar, M., Chaumont, D., Lacroute, Y., Patriarche, G., Gomez, M.E., Zambrano, G., Sacilotti, M., 2008. Phys. Status Solidi 205(2), 289-293.

Li, G., Tang, Z., 2014. Nanoscale 6(8), 3995-4011.

Lima, V.L.M., Correia, M.T.S., Cechinel, Y.M.N., Sampaio, C.A.M., Owen, J.S., Coelho, L.C.B.B., 1997. Carbohyd. Polym. 33(1), 27-32.

Liu, Y., Zhu, F., Dan, W., Fu, Y., Liu, S., 2014. Analyst 139(20), 5086-5092.

Liu, Z., Liu, H., Wang, L., Su, X., 2016. Anal. Chim. Acta 932 88-97.

Lloyd, K.O., Burchell, J., Kudryashov, V., Yin, B.W.T., TaylorPapadimitriou, J., 1996. J. Biol. Chem. 271(52), 33325-33334.

Lucarelli, F., Tombelli, S., Minunni, M., Marrazza, G., Mascini, M., 2008. Anal. Chim. Acta 609(2), 139-159.

Luna, D.M.N., Avelino, K.Y.P.S., Cordeiro, M.T., Andrade, C.A.S., Oliveira, M.D.L., 2015. Sens. Act. B: Chem. 220, 565-572.

Meany, D.L., Zhang, Z., Sokoll, L.J., Zhang, H., Chan, D.W., 2009. J. Proteome Res. 8(2), 613-619.

Mody, R., Joshi, S., Chaney, W., 1995. J. Pharmacol. Toxicol. 33(1), 1-10.

Mulder, A., Huskens, J., Reinhoudt, D.N., 2004. Org. Biomol. Chem. 2(23), 3409-3424.

Nyikos, L., Pajkossy, T., 1985. Electrochim. Acta 30, 1533.

Oliveira, M.D., Andrade, C.A.S., Correia, M.T.S., Coelho, L.C.B.B., Singh, P.R., Zeng, X., 2011. J. Coll. Int. Sci. 362(1), 194-201.

Oliveira, M.D.L., Correia, M.T.S., Coelho, L.C.B.B., Diniz, F.B., 2008. Coll. Surf. B 66(1), 13-19.

Pajkossy, T., 1997. Sol. State Ionics 94, 123.

Pan, C., Guo, M., Nie, Z., Xiao, X., Yao, S., 2009. Electroanal. 21(11), 1321-1326.

Pellegrini, R., Mariotti, A., Tagliabue, E., Bressan, R., Bunone, G., Coradini, D., Della Valle, G., Formelli, F., Cleris, L., Radice, P., 1995. Cell Growth Differ 6(7), 863-869.

Petrelli, F., Coinu, A., Borgonovo, K., Cabiddu, M., Ghilardi, M., Lonati, V., Barni, S., 2014. Breast Cancer Res. Treat. 144(2), 223-232.

Sadik, O.A., Yan, F., 2007. Anal. Chim. Acta 588, 292-296.

Sage, A.T., Besant, J.D., Lam, B., Sargent, E.H., Kelley, S.O., 2014. Acc. Chem. Res. 47(8), 2417-2425.

Samoszuk, M., Tan, J., Chorn, G., 2005. Breast Cancer Res. 7(3), R274- R283.

Simão, E.P., Barbieri, G.J.L.S., Andrade, C.A.S., Oliveira, M.D.L., 2016. J. Braz. Chem. Soc. 27, 1040-1047.

Subramanian, V., Wolf, E.E., Kamat, P.V., 2004. J. Amer. Chem. Soc. 126(15), 4943-4950.

Tepeli, Y., Barlas, F.B., Timur, S., Anik, U., 2016. Electrochim. Acta 211, 71-76.

Tepeli, Y., Demir, B., Timur, S., Anik, U., 2015. RSC Adv. 5(66), 53973-53978.

Thiagarajan, V., Madhurantakam, S., Sethuraman, S., Balaguru Rayappan, J.B., Maheswari Krishnan, U., 2016. J. Coll. Interf. Sci. 462, 334-340.

Tong, X., Benz, L., Chrétien, S., Metiu, H., Bowers, M.T., Buratto, S.K., 2010. J. Phys. Chem. C 114(9), 3987-3990.

Tsay, G.C., Dawson, G., Matalon, R., 1975. J. Clin. Invest. 56, 711-718.

van Gisbergen, K.P.J.M., Aarnoudse, C.A., Meijer, G.A., Geijtenbeek, T.B.H., van Kooyk, Y., 2005. Cancer Res. 65(13), 5935-5944.

Varki, A., Schauer, R., 2009. Sialic acids. In: Varki A, Cummings RD, Esko JD, Freeze HH, Stanley P, Bertozzi CR, Hart GW, Etzler ME, editors. Source Essentials of Glycobiology. 2nd edition. Cold Spring Harbor (NY): Cold Spring Harbor Laboratory Press; 2009. Chapter 14.

Wang, Y.G., Yoon, Y., Glezakou, V.A., Li, J., Rousseau, R., 2013. J. Amer. Chem. Soc. 135(29), 10673-10683.

Yang, H., Li, Z., Shan, M., Li, C., Qi, H., Gao, Q., Wang, J., Zhang, C., 2015. Anal. Chim. Acta 863, 1-8.

Zajchowski, D.A., Bartholdi, M.F., Gong, Y., Webster, L., Liu, H.-L., Munishkin, A., Beauheim, C., Harvey, S., Ethier, S.P., Johnson, P.H., 2001. Cancer Res. 61(13), 5168-5178.

Zhang, X., Teng, Y., Fu, Y., Xu, L., Zhang, S., He, B., Wang, C., Zhang, W., 2010. Anal. Chem. 82(22), 9455-9460.

Highlights

- A three-dimensional-based biosensor platform was obtained.
- We successfully made a distinction between highly and less invasive cancer cell lines.
- The proposed approach demonstrated detection limits as low as 10 cells/mL.
- The proposed platform could be useful to facilitate the medical diagnosis of the cancer.

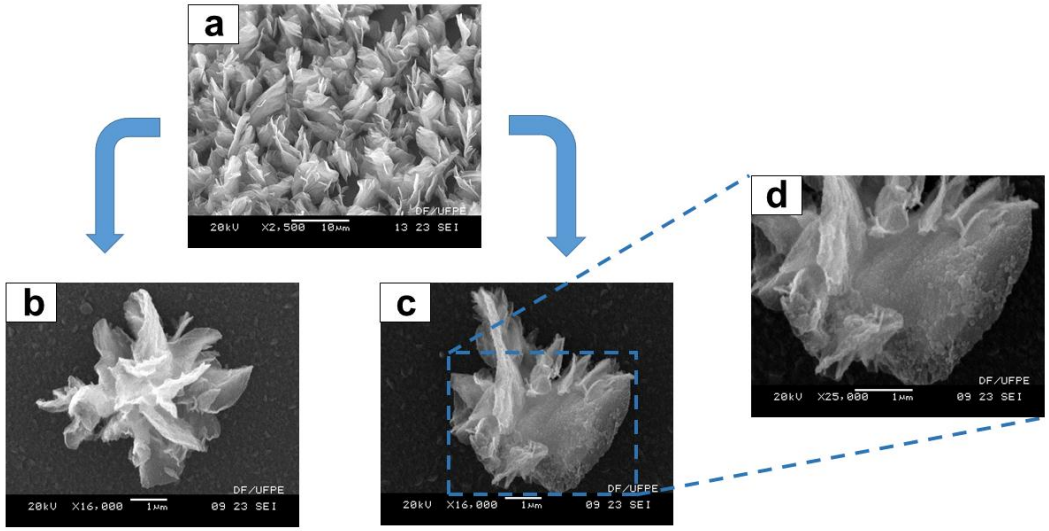

ConA-MCF7

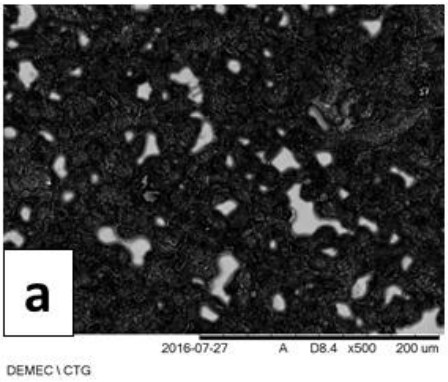

WGA-MCF7

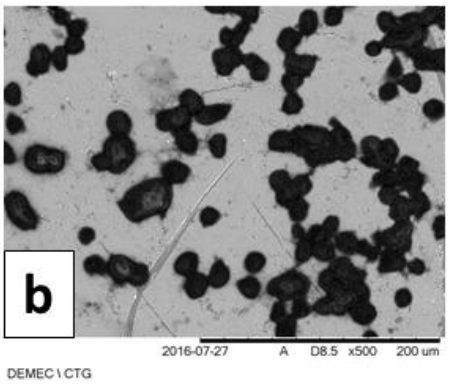

ConA-T47D

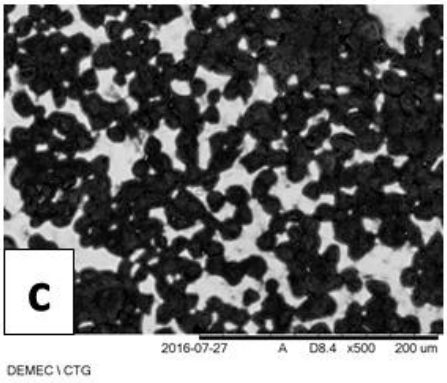

WGA-T47D

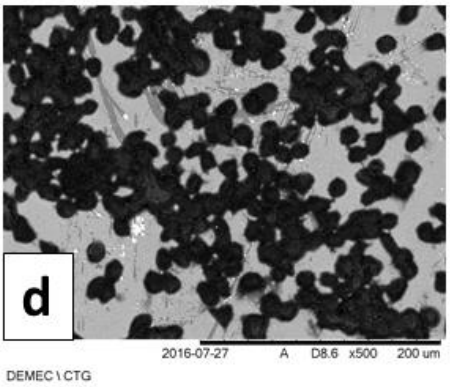

ConA-NHSF

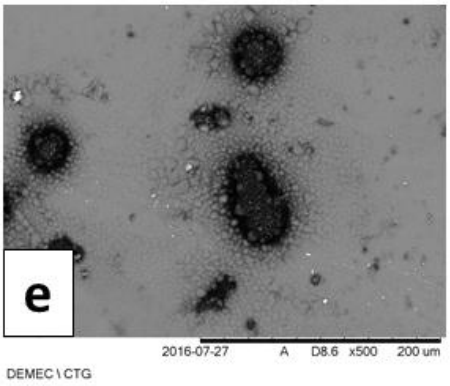

WGA-NHSF

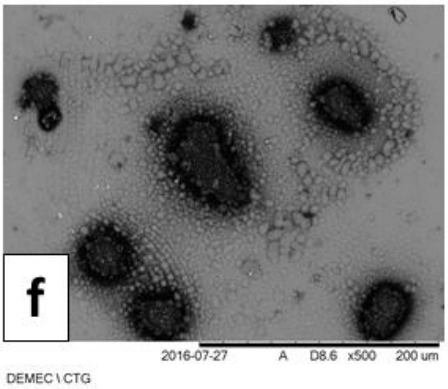

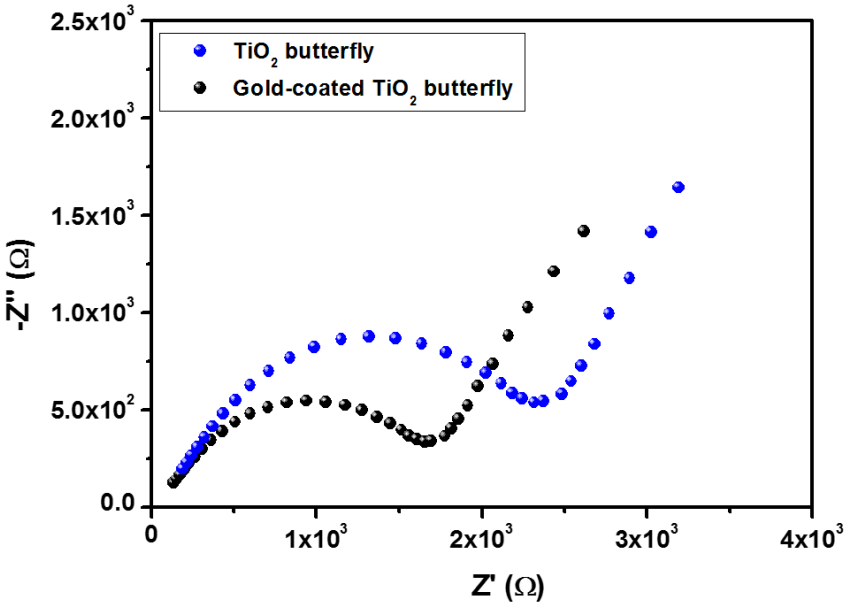

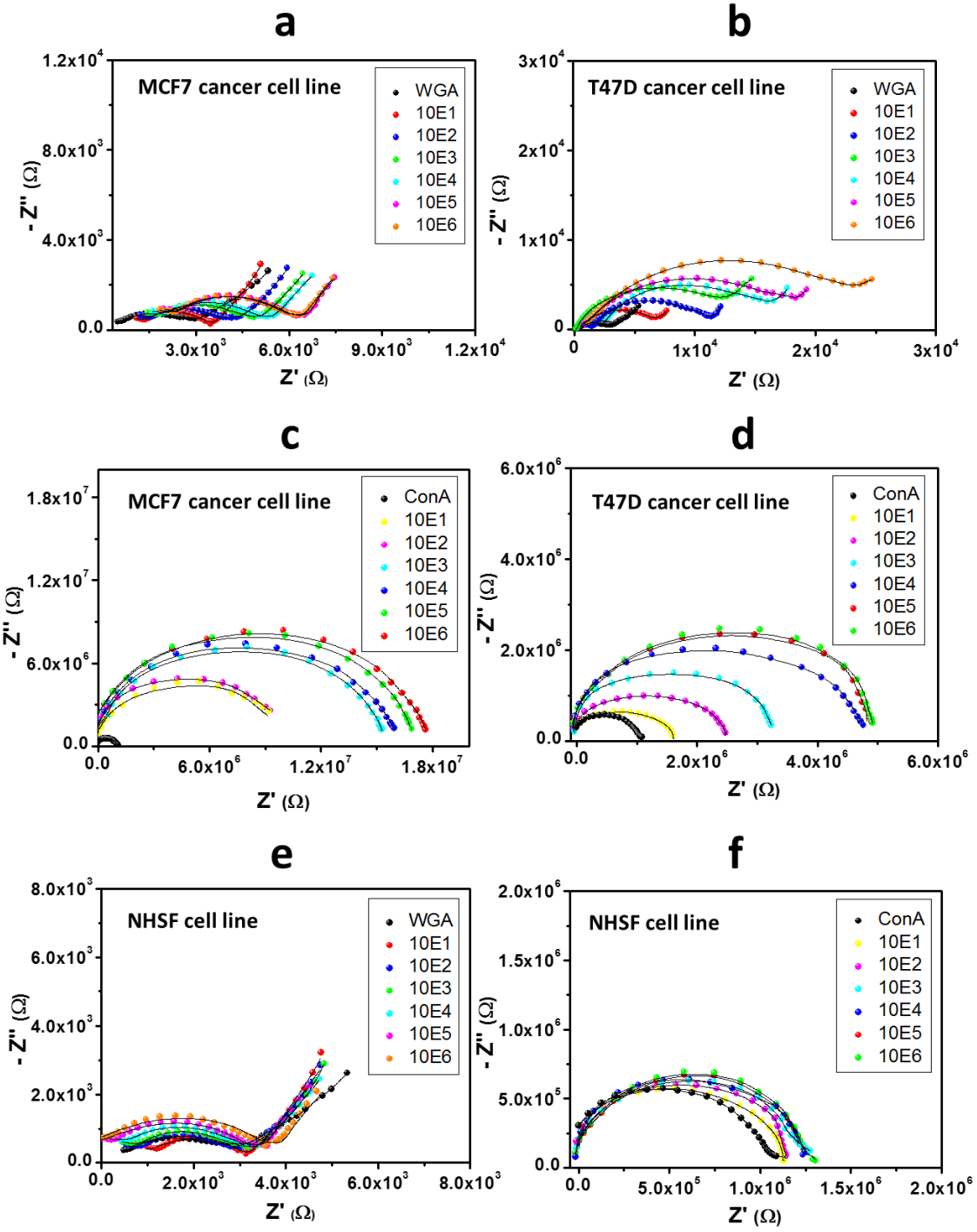
a
MCF7 cancer cell line
WGA
10E1
10E2
10E3
10E4
10E5
10E6
- Z'' (Ω)
Z' (Ω)
b
T47D cancer cell line
WGA
10E1
10E2
10E3
10E4
10E5
10E6
- Z'' (Ω)
Z' (Ω)
c
MCF7 cancer cell line
ConA
10E1
10E2
10E3
10E4
10E5
10E6
- Z'' (Ω)
Z' (Ω)
d
T47D cancer cell line
ConA
10E1
10E2
10E3
10E4
10E5
10E6
- Z'' (Ω)
Z' (Ω)
e
NHSF cell line
WGA
10E1
10E2
10E3
10E4
10E5
10E6
- Z'' (Ω)
Z' (Ω)
f
NHSF cell line
ConA
10E1
10E2
10E3
10E4
10E5
10E6
- Z'' (Ω)
Z' (Ω)